Design and Characterization of Purely Textile Patch Antennas

Ivo Locher, *Student Member, IEEE*, Maciej Klemm, *Student Member, IEEE*, Tünde Kirstein, and Gerhard Tröster, *Senior Member, IEEE*

***Abstract*—In this paper, we present four purely textile patch antennas for Bluetooth applications in wearable computing using the frequency range around 2.4 GHz. The textile materials and the planar antenna shape provide a smooth integration into clothing while preserving the typical properties of textiles. The four antennas differ in the deployed materials and in the antenna polarization, but all of them feature a microstrip line as antenna feed. We have developed a manufacturing process that guarantees unaffected electrical behavior of the individual materials when composed to an antenna. Thus, the conductive textiles possess a sheet resistance of less than $1\Omega/\square$ in order to keep losses at a minimum. The process also satisfies our requirements in terms of accuracy meeting the Bluetooth specifications. Our investigations not only characterize the performance of the antennas in planar shape, but also under defined bending conditions that resemble those of a worn garment. We show that the antennas can withstand clothing bends down to a radius of 37.5 mm without violating specifications.**

***Index Terms*—Fabric antennas, conductive textiles, fabric substrates, wearable computing.**

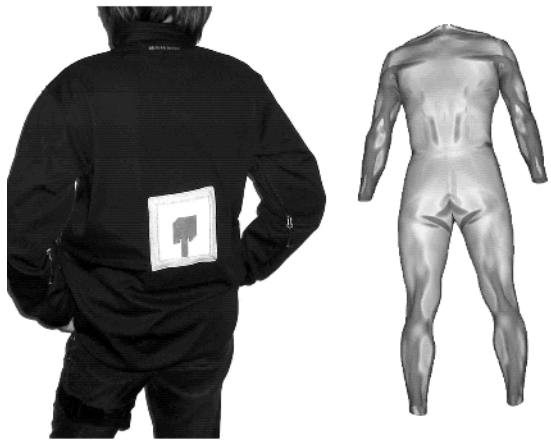

Fig. 1. Textile patch antenna on the human body. (a) Mounted textile patch antenna for a Bluetooth WPAN. (b) Curvature radii along the human body.

I. Introduction

WEARABLE computing is a fast growing field in application-oriented research. Steadily progressing miniaturization in microelectronics along with other new technologies enables integration of functionality in clothing allowing entirely new applications. The vision of wearable computing describes future electronic systems as an integral part of our everyday clothing serving as intelligent personal assistants. A wearable computer is always on, does not restrict the user's activities and is aware of the user's situation. It features easy-to-use interfaces and supports him unobtrusively with *in situ* information [1]. An important ingredient of such a system is the connection to a wireless personal area network (WPAN). For this purpose, we propose the use of purely textile antennas that guarantees flexible and comfortable embedding into clothing as depicted in Fig 1(a). A flexible embedding is important since bending radii as small as 10 mm can occur in garments along the body, especially around joints. Fig. 1(b) qualitatively shows the curvature distribution along the human body. The darker a region appears, the smaller the radius is. A curvature on a human body consists of a superposition of bends in arbitrary directions. Only textiles can follow these exposures. This property is called *Drapability*. In contrast, a flexible PCB substrate such as polyamides allows bending only in a single direction at a time. The material prohibits a superposition of bends. Our textile antennas for wearable applications withstand such bending stresses while maintaining their radiation specifications.

In this paper, we present four textile patch antennas for Bluetooth [2] in the frequency range from 2400 to 2483.5 MHz. Our antennas feature a 10-dB bandwidth of 200 MHz on average. Even when bent around a radius of 37.5 mm resembling a mounting on a human upper arm, Bluetooth specifications can be assured. The planar structure with a maximal thickness of 6 mm maintains wearing comfort when integrated into clothing. In contrast to a probe feed, our microstrip feedline does not increase the height of the patch antennas. The fundamental composition of a patch antenna is shown in Fig. 2. More information about antennas including an overview of antenna specific terms is given in [3].

Using a microstrip feed not only guarantees a flat structure, but also allows the assembly of electronic components directly on the fabric in antenna proximity. By applying a similar technology as described in [4], autonomous systems with only few nontextile components are feasible.

Prior to the antenna design, we carried out systematic investigations regarding the electrical performance of the deployed materials, i.e., the conductive textiles and the fabric substrates.

Manuscript received January 12, 2006; revised April 14, 2005 and May 22, 2006.

I. Locher was with the Electronics Laboratory and the Wearable Computing Laboratory, Department of Information Technology and Electrical Engineering, Swiss Federal Institute of Technology (ETH) Zürich, 8092 Zürich, Switzerland. He is now with Sefar, Inc., 8803 Rüschlikon, Switzerland (e-mail: ivo.locher@sefar.ch).

M. Klemm, T. Kirstein, and G. Tröster are with the Electronics Laboratory and the Wearable Computing Laboratory, Department of Information Technology and Electrical Engineering, Swiss Federal Institute of Technology (ETH) Zürich, 8092 Zürich, Switzerland .

Digital Object Identifier 10.1109/TADVP.2006.884780

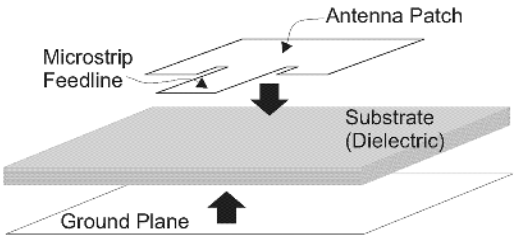

Fig. 2. Composition of a patch antenna with microstrip feedline.

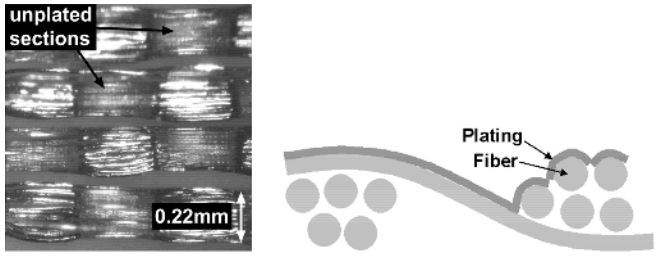

Fig. 3. (a) Nickel-plated fabric. (b) Cross-section drawing.

We were interested in the electrical resistance of the conductive textiles, its homogeneity, and its behavior under elongation stress as well as the skin depth in the frequency range around 2.4 GHz. Second, we determined the permittivity of the fabric substrates in the same frequency range with regard to the humidity level.

Two of the four antennas feature linear polarization and two of them possess left-handed circular polarizations (LHCP). Our goal was to explore the tradeoffs between electrical performance and maintaining textile properties. Because of the flexible nature of textiles, we not only characterized the antennas in planar shape, but also under defined bending conditions that resemble those of a worn garment. In the following sections, we will also comment on interesting textile-specific problems we encountered during the design process.

II. Related Work

Most existing wearable computers still consist of bulky and rigid boxes and are portable rather than wearable. Some approaches have been made to integrate electronic components into clothing, but usually the textile itself just serves as a carrier of conventional electronics. Another approach is to use textiles for electrical functions such as transmission lines and sensors. First, systematic studies of electrical properties of textile transmission lines were carried out by Cottet *et al.* [5]. They proved that signals with a bandwidth of more than 100 MHz can be transmitted over textile transmission lines using wire pair configuration.

The next step was the development of packaging and assembly technologies for electronic components in order to enable electrical circuits in textiles [4].

Wearable antennas presented by Salonen [6] and Massey [7] are partially based on textiles possessing an inverted-F shape that results in a stiff structure. Other textile antennas described by Tanaka *et al.* [8] and Salonen *et al.* [9] are designed as rectangular patches with probe feed and linear polarization. Antennas such as presented in [10] only utilize fabrics as substrate, whereas the patches and ground planes are copper foils.

In this paper, we advanced our work presented in [11] by applying materials with better electrical performances and by new methods for fabrication of the antennas. All antennas provide a microstrip feedline, whereas two antennas feature linear polarization and two antennas feature left-handed circular polarization. Furthermore, we conducted more rigorous simulations and measurements on the antennas regarding their performance in planar shape as well as under bending.

III. Textile Materials

Planar antenna structures are generally favored in wearable applications since they can easily be integrated in clothing. Inspired by the simple buildup of printed microstrip antennas, we adapted this technology to textiles. Therefore, we needed an electrically conductive fabric for the ground planes as well as for the antenna patches. Second, we required a fabric substrate with constant thickness and stable permittivity. An accurate determination of the electrical parameters for the fabrics (dielectric substrate and conductive textile) is crucial for correct antenna simulations and agreement with measurements.

A. Electrically Conductive Fabric

For the purpose of a textile antenna design, a conductive fabric needs to satisfy the listed requirements below. The closer a fabric meets the requirements the better performs the antenna.

- A low and stable electrical resistance ($\leq 1\Omega/\square$) of the fabric is desired to minimize losses
- The (sheet) resistance must be homogeneous over the antenna area. In other words, the variance of the resistance must be small.
- The fabric should be flexible such that the antenna can be deformed.
- A stretchable fabric supports the deformation behavior of an antenna.

An electrical resistance of $\leq 1\Omega/\square$ is a reasonable choice for conductive fabrics. From an electrical point of view, we would recommend using copper foils. However, such foils lack of drapability and elasticity that limits their use in clothing.

Among the many fabrics, we chose three variants for further investigations concerning the stated requirements

1) a no-name nickel-plated woven fabric (the plating thickness is about 250 nm);
2) a silver plated knitted fabric [12];
3) a silver–copper–nickel plated woven fabric [13].

1) Nickel-Plated Fabric 1): Although nickel shows excellent resistance against corrosion, the nickel-plated fabric 1) turned out to be not suitable for antenna applications since the plating was applied after weaving process. Thus, the woven fibers are not entirely plated where they cross each other. Fig. 3 shows the fabric with removed weft fiber (vertical yarn). The unplated sections can be recognized easily. As a result, a single fiber is not continuously conductive. The electrical current cannot flow along a single fiber, but instead must "hop" from wrap fiber to weft fiber and vice versa over a very small overlapping plating of crossing fibers. These transitions from fibers to fibers are the

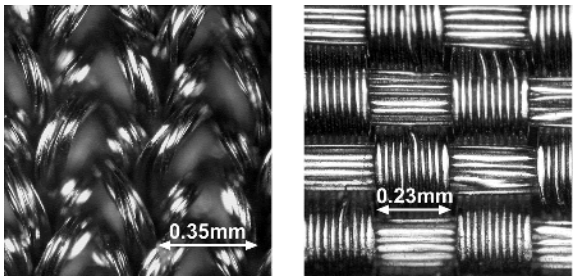

Fig. 4. (a) Conductive, knitted P130 $\uparrow y$, $\rightarrow x$ and (b) woven Nora fabric.

TABLE I
PROPERTIES OF CONDUCTIVE KNITTED AND WOVEN FABRIC

Property	Knitted (2)	Woven (3)
Fabric thickness	$0.55mm \pm 10\%$	$0.15mm$
Yarn polymer	Polyamide	Polyamide
Yarn / thread pitch	$0.35mm$	$0.23mm$
Fibers per yarn	6	12
Weight	$180g/m^2$	$72g/m^2$
Plating	Ag	Ni / Cu / Ag
Sheet resistance	$< 1\Omega/\square$	$0.02\Omega/\square$
Equivalent Ag thickness	$16.3nm$	$815nm$

main reason for the sheet resistance of about $5\Omega/\square$. Additionally, measurements showed that the sheet resistance is inhomogeneous over the area.

As a consequence, we focused on the other two conductive fabrics (2 and 3) for the antenna design. The fibers of these fabrics were plated before weaving and knitting, respectively. Therefore, their sheet resistance is much better as shown in Table I, though still caused by the fiber-to-fiber transition resistance mainly. For comparison, Table I also gives the equivalent thickness of a pure silver foil to achieve equal conductivity as the fabric. Pictures of the fabrics can be seen in Fig. 4.

2) Silver-Plated Knitted Fabric 2): The fabric consists of entirely plated polyamide fibers. Given by the nature of knitting, fabric 2) is viscoelastic featuring an approximated Young's modulus of $E = 150$ kPa at elongations of more than 30%. Regarding mechanical properties, an antenna composed of this fabric is bendable and, therefore, it can comfortably be integrated into clothing since the fabric elongates where necessary. From a manufacturing point of view, the elasticity is a drawback because precise shaping as well as assembly of the antenna without warpage is difficult. The antenna shapes manufactured finally achieved a geometrical accuracy of about ± 0.5 mm. The warpage and bending have, of course, influence on the antenna characteristics, i.e., S_{11}. Second, they affect the sheet resistance due to strain stress. We measured this resistance change depending on elongation (and strain stress) in the x- and y-direction, which is shown in Fig. 5. Since the knitting possesses a column-like structure [see Fig. 4(a)], the resistance behavior differs in the orthogonal axes (inhomogeneity). Elongation in the y-axis has only a minor effect on the resistance, whereas the resistance increases significantly when elongated in the x-axis. Both curves progress linearly for small elongations and flatten out for larger elongations. This behavior is not yet entirely understood. It will supplementary perturb the antenna characteristic in case of bending, especially when bending results in a

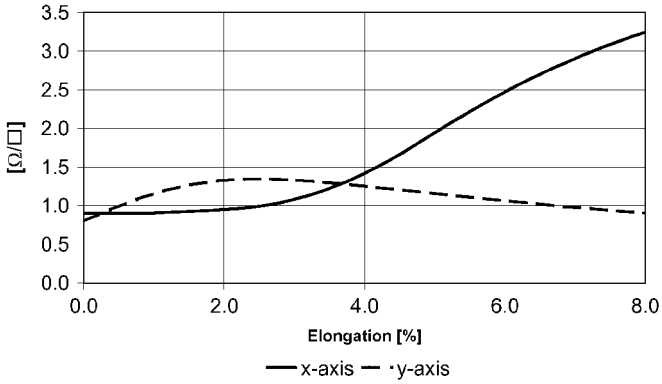

Fig. 5. Sheet resistance change due to elongation of the knitted fabric 2).

stretch in the x-axis. In fact, the value given in Table I is valid for a zero-force strain. Furthermore, relaxation after a stretching of 10% lasts about 20 s. Thus, fast cycles between strain stress and release result in a hysteresis regarding geometrical dimensions as well as sheet resistance.

This material satisfies all the stated requirements but homogeneity in resistance when bent.

3) Silver-Copper–Nickel-Plated Woven Fabric 3): Compared to the knitted fabric 2), fabric 3) features low elasticity due to its woven structure [see Fig. 4(b)]. In contrast to fabric 1), the fibers of fabric 3) are plated before weaving resulting in a low electrical resistance (Table I). The Young's modulus of about 2.4 GPa is mainly determined by the polyamide material of the thread in fabric 3). Therefore, its shape can be manufactured precisely, but bending of such an antenna is then limited. Additionally, the edges of this fabric tend to fray easily due to the nature of woven fabric. This effect can be minimized by using manufacturing techniques explained in Section V. In conclusion, the woven fabric possesses the best electrical properties among the three fabrics to build well-behaved antennas with geometrical accuracies of about ± 0.15 mm.

Shape Precision of the Conductive Fabrics: The woven antenna patch can only be shaped with the finite precision given by the thread thickness. In fact, the thread pitch virtually "discretizes" the possible sizes of the conductive patches. Assuming an antenna patch consists of N threads in one direction. The patch width then corresponds to N times thread pitch. Notice that the next possible width of the patch is either $(N+1)$ times thread pitch or $(N-1)$ times thread pitch.

In case of the knitted antenna patch, instable dimensions due to elasticity of the fabric limit precision.

Plating Thickness: The targeted frequency range (2.4 GHz) features a theoretical skin depth of about 1.3μm given by (1), where Ag plating is assumed. Thus, the skin effect increases electrical resistance that causes additional losses. Moreover, the plating thickness of the fabrics is restricted to several hundred nanometers in order to maintain textile properties. This fact again increases damping in the final antenna occluding the skin effect. The impact of this effect is illustrated in Section VI:

$$\delta = \frac{1}{\sqrt{\pi f \mu \sigma}} \quad [m] \tag{1}$$

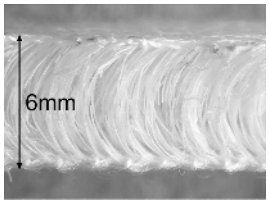

Fig. 6. Cross section of spacer fabric substrate.

where δ is skin depth, f is frequency, μ is magnetic permeability, and σ is electrical conductivity.

B. Textile Substrates

The textile substrate provides the dielectric between the antenna patch and the ground plane (see Fig. 2). It requires constant thickness of few millimeters and low permittivity such that the antenna patch becomes large and effects of absolute tolerances in geometry diminish. Thus, we target a relative tolerance of about 3% corresponding to the accuracy given in Section III-A.

We chose a woolen felt with a thickness of 3.5 mm and a polyamide spacer fabric with a thickness of 6 mm as substrates. The felt with a density of 1050 g/m^2 is dimensionally more stable and harder to bend, whereas the spacer fabric with 530 g/m^2 is lighter and elastic due to its knitting-based structure. Furthermore, the spacer fabric can easily be compressed as might intuitively be guessed by looking at Fig. 6. Nevertheless, the fabric totally recovers after release of the load. Such a fabric can be integrated in jackets as depicted in Fig. 1(a) and function as thermal insulation simultaneously.

We used techniques explained by Grzyb *et al.* in [14] in order to extract the permittivity of the textile substrates. This method utilizes scattering parameter measurements of two microstrip transmission lines of different lengths. As a result, connection discontinuities in the measurement setup can be eliminated by computation. Finally, a permittivity $\epsilon_r = 1.45 \pm 0.02$ for the felt and $\epsilon_r = 1.14 \pm 0.025$ for the spacer fabric was extracted at a frequency of 2.4 GHz. The loss tangent of the felt is $\tan\delta = 0.02$, whereas the loss tangent of the spacer fabric is negligible. Extensive humidity measurements covering a range from 20%RH to 80%RH within a temperature range of 25 °C to 80°C showed that permittivity variations are negligible compared to the measurement uncertainty. This result closely corresponds to the numbers given in [15] for the humidity effect on the permittivity of air since both substrate permittivities are close to 1.

In contrast, flexible substrates such as polyamide and liquid crystalline polymers (LCP) are foils. Therefore, they lack drapabilty and are only bendable in one direction at a time. This textile-atypical behavior of foils is a major drawback for integration into clothing.

C. Clothing Deformation

We defined two bending radii for the antennas aiming the mounting on arms and legs in wearable applications. The effects of bending on the electrical performance of antennas can be seen in Section VI. Geometrically, the elongation Δw is connected with the bending radius R according to (2) and Fig. 7 assuming constant material thickness and a centered neutral phase. These assumptions are approximately valid for the knitted fabric, whereas the inelasticity of the woven fabric merely causes a small dent in the substrate. In other words, the knitted fabric follows the curve of the bending while the woven fabric stays straight:

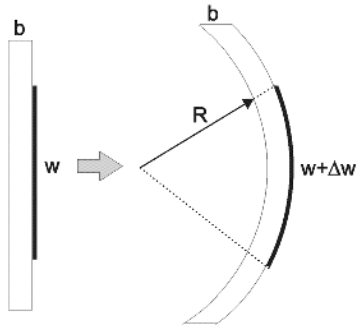

Fig. 7. Patch elongation due to bending.

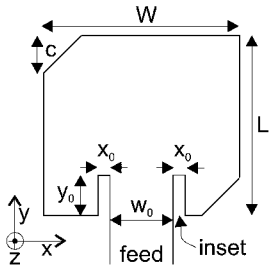

Fig. 8. Patch antenna sketch.

$$\frac{\Delta w}{w} = \frac{b}{2R+b} \tag{2}$$

IV. Antenna Design

A. Theory and Simulation

Targeting wearable applications, a planar structure of the antenna is important, but also is a planar antenna feed. Thus, we discarded probe feeds, which actually eases the antenna design. Instead, we use microstrip feed lines. In the design of the microstrip antenna patches, transmission line model equations (3) and (4), such as given in Balanis [16], were applied for a rough estimate. The correspondence of the formula symbols to the actual antenna shape is shown in Fig. 8. f_r is the resonance frequency of the antenna, and ΔL is the extended distance of the principal E-plane. For further information, please consult Balanis [16]:

$$W = \frac{1}{2 \cdot f_r \sqrt{\mu_0 \epsilon_0}} \sqrt{\frac{2}{\epsilon_r + 1}} \quad [m] \tag{3}$$

$$L = \frac{1}{2 \cdot f_r \sqrt{\epsilon_{r_{eff}} \mu_0 \epsilon_0}} - 2 \cdot \Delta L \quad [m]. \tag{4}$$

We chose a 75-Ω microstrip feed line for the spacer fabric since a 50-Ω line would become about 28 mm wide, leading to

TABLE II
DESIGNED ANTENNA VARIANTS AND MATERIALS

Antenna name	Substrate	Substrate height	Conductive material	Polarization	Feed line Z_0
LF	felt	$3.5mm$	knitting (2)	linear	50Ω
CF	felt	$3.5mm$	knitting (2)	circular	50Ω
LS	spacer	$6mm$	knitting (2) & woven (3) *	linear	75Ω
CS	spacer	$6mm$	woven (3)	circular	75Ω

* knitted antenna patch / woven ground plane

TABLE III
DIMENSIONS OF THE FOUR ANTENNAS INCLUDING TOLERANCES [MILLIMETERS]

Dimension	LF	CF	LS	CS
W	64	44	58	47
L	49	51	53	57
c	0	8.5	0	8
y_0	13	8	14	9
x_0	1	3	3	3
w_0	14	14	14	14
Tolerance	± 0.5	± 0.5	± 0.5	± 0.15

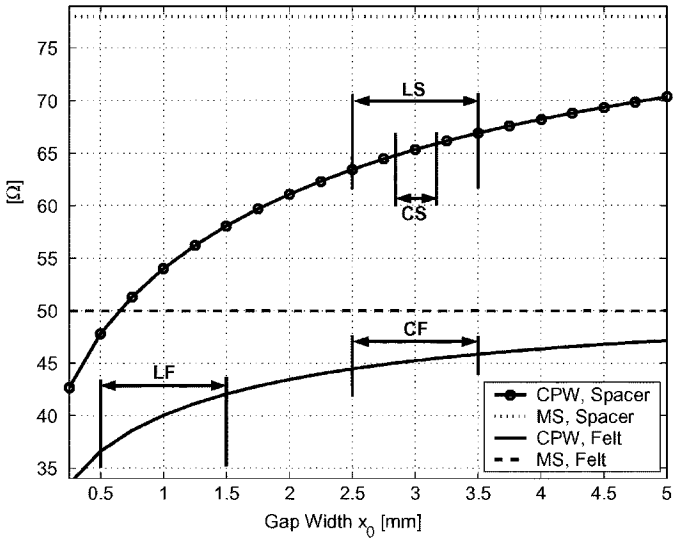

Fig. 9. Characteristic impedances of CPWs w.r.t gap width x_0 ($w_0 = 14$ mm) including manufacturing tolerances indicated by arrows.

a disturbed radiation characteristic of the antenna. On the other hand, a 50-Ω microstrip feed line was used for the felt substrate with its higher permittivity. To avoid losses due to mismatch between feed line and antenna, we have applied commonly known techniques described in [17]. There, insets along the feed line are incorporated into the antenna patch in order to adjust the antenna's input impedance (Fig. 8). The width w_0 of the microstrip feed to meet 50-Ω and 75-Ω line impedance, respectively, were computed using the standard formulas given in Balanis [16] as well.

Having a first estimate by applying the aforementioned techniques, we performed full-wave electromagnetic simulations using Ansoft HFSS [18] to improve our antenna design.

We designed the four antennas (two linearly and two circularly polarized) listed in Table II with their dimensions in Table III. The truncated corners c in Fig. 8 introduce circular polarization, in our case LHCP.

It is worth mentioning that a thinner substrate would increase the effective permittivity $\epsilon_{r_{\text{eff}}}$ and, therefore, decrease the size of the antenna. On the one hand, this fact is beneficial regarding antenna integration into clothing. Second, 50-Ω impedance can be achieved even for low-permittivity material. With a substrate thickness of 1 mm, the width of a 50-Ω feed line would shrink to 3.5 mm for the felt and to 4 mm for the spacer fabric.

On the other hand, the absolute tolerances do not change and, therefore, manufacturing of a textile antenna with the intended properties is critical outlined in Section III.

B. Antenna Insets

During the design process and first implementations, we noticed the importance of an accurate transition from microstrip feed line to the antenna patch. Whereas accuracies better than 1 μm are achievable in PCB manufacturing, tolerancies for textiles lie in the range of 0.5 mm as explained in Section III. Second, the feed to the antenna has microstrip configuration (MS); however, as soon as the insets begin, it more resembles a finite-width conductor backed coplanar waveguide structure (FW-CBCPW), i.e., a microstrip line surrounded with ground planes. Fig. 9 shows the characteristic impedance of coplanar waveguides (CPW) with respect to the gap width between trace and these ground planes for the two textile substrates. In our context, the gap width of the CPW corresponds to the inset width x_0 of the antenna. As expected, the impendance asymptotically approaches an upper bound given by the impedance of the microstrip line (MS), where the ground planes on the microstrip line side can be assumed as infinitely far away. A constant trace width of $w_0 = 14$ mm was assumed in Fig. 9. The shape of the curve further implies that variations, e.g., imprecision in manufacturing, have bigger impacts on the impedance when the gap width is small. Fig. 9 also indicates the impedance range of the feedlines due to manufacturing tolerances for the four antennas. This span is determined by the conductive textile materials (see Section III-A) whereas its location is given by the antenna design. For instance, the CPW of the CS antenna features smaller tolerances than the CPW of the LS antenna since it is made of the woven fabric.

In conclusion, wide insets x_0 smooth out the transition from MS to CPW antenna inset regarding impedances. Second, the CPW impedance curve flattens out for wide insets that introduce higher robustness against dimensional tolerances due to manufacturing and deformation of the antenna.

V. ANTENNA MANUFACTURING

In the antenna manufacturing process, the composition of the conductive antenna patch with the dielectric substrate is critical. First of all, the dimensions of the patch must be retained while being attached to the substrate. Second, the attachment procedure must not affect the electrical properties of the patch, e.g., the sheet resistance. For composition, we evaluated the following four methods:

1) liquid textile adhesive (brand: Golden Fix);
2) point-wise application of conductive adhesives;
3) sewing;
4) adhesive sheets, which are activated by ironing.

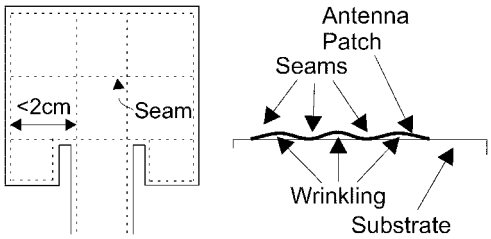

Fig. 10. Sewed antenna. (a) Sewed antenna patch with seam grid. (b) Wrinkling of antenna patch between seams (cross section).

Application of the liquid textile adhesive 1) on conductive fabrics showed soaking effects such that distribution of an evenly thin film of adhesives was impractical. As a result, the adhesive acts as insulator among the conductive yarns. Because of the uneven distribution, electrical resistance showed inhomogeneity, and it could rise by a factor of ten at certain spots.

A point-wise deposition of conductive adhesive 2) in a 1-cm spacing did not increase the sheet resistance; however, mechanical stability was significantly worse compared to the textile adhesive 1). Second, accurate attachment of the antenna patch was not ensured in terms of preserving geometry. Conductive adhesives cannot be applied in an area-wide manner on textiles since these types of adhesives usually are stiff and brittle.

Similarly for sewing 3), attention needs to be paid preventing warpage during the sewing process. Second, the seam spacing must be smaller than 2 cm in order to minimize wrinkling. This behavior is illustrated in Fig. 10. A wrinkling corresponds to uneven distances between the antenna patch and the ground plane resulting in distortion of the antenna characteristic. A stitch passes through both the patch and the ground plane of the antenna. Electrical measurements revealed shorts between antenna patch and ground plane because the sewing needle pulled small conductive fibers from the patch through the substrate and shorted them with the ground plane. Besides, sewing could not be used with the spacer fabric substrate since the high pressure of the sewing seam compressed the substrate permanently.

The adhesive sheets 4) show the best results. It evenly deposits as a thin layer on the conductive textile by ironing. Moreover, the adhesive only penetrates the surface of the conductive textile such that patch sheet resistance and substrate permittivity are not changed.

Nevertheless, maintaining of the geometrical dimensions needs to be guaranteed during attaching of the conductive antenna patch to the substrate. The knitted fabric is particularly challenging because it tends to curl. Therefore, we deploy a temporary stabilization and stiffening of the fabric until after its attachment. This is done by application of a water-soluble foil to the fabric. After ironing of the stiff conductive fabric onto the substrate, the foil can entirely be dissolved in water.

From the mechanical point of view, the spacer fabric substrate too is elastic and stretchable because it is based on knitting as well (see Fig. 6). By stretching the substrate, a knitted antenna patch [fabric 2)] can be varied by several millimeters resulting in a big change of the antenna characteristic. As a consequence, we utilize a patch of non-elastic conductive woven fabric [fabric 3)] for mechanical stabilization of the spacer fabric. In the case of the linearly polarized antenna with spacer fabric substrate (LS antenna), a woven ground plane fulfilled our demands, whereas we had to apply the woven fabric for both the antenna patch and the ground plane in the case of the circularly polarized antenna with spacer fabric substrate (CS).

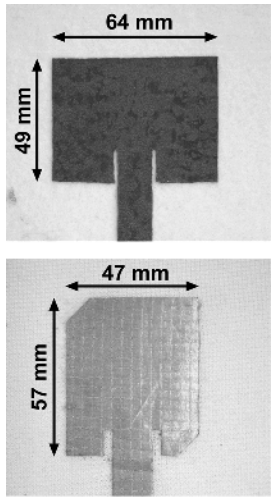

Fig. 11. Two of the four antennas manufactured (top view) (a) LF antenna. (b) CS antenna.

Finally, we achieved textile antennas with accurate shapes, good mechanical stability as well as stable and low sheet resistance by utilization of adhesive sheets and water-soluble foil along with suitable conductive fabrics. Two of the four antennas are shown for illustration in Fig. 11.

VI. Antenna Simulation and Measurement Results

In this section, we compare the simulated antenna characteristics with the measurements conducted in the anechoic chamber. For the antennas, we show S_{11} (input reflection coefficient), radiation pattern and for the circularly polarized variants (CP) the axial ratio. We further discuss the effect of material choice on the gain at a particular antenna. Second, we carried out measurements with the antennas bent around cylinders (see Section VI-A) in order to investigate their potential behavior in wearable applications. Special attention was also paid to the interconnect between measurement equipment and fabric antenna. Due to modeling of this connection using Ansoft HFSS [19], we could deduct its effect from the S_{11} measurements.

A. Antenna Bending Gauge

The bending gauge must not affect the measured antenna characteristic. Hence, we chose a thin-walled PVC (dielectric constant between 4 and 5) pipe with additional drilled holes such that the amount of air is maximized. S_{11} measurements of the antennas mounted on this pipe showed minor differences to measurements on a solid pipe proofing that the PVC pipe minimally effects the antenna characteristic. Second, by using pipes in contrast to just folding the antennas as conducted by Tanaka *et al.* in [8], we can guarantee a well-defined bending radius and therefore reproducibility. The radii for bending were chosen to be 37.5 and 100 mm, respectively, corresponding approximately

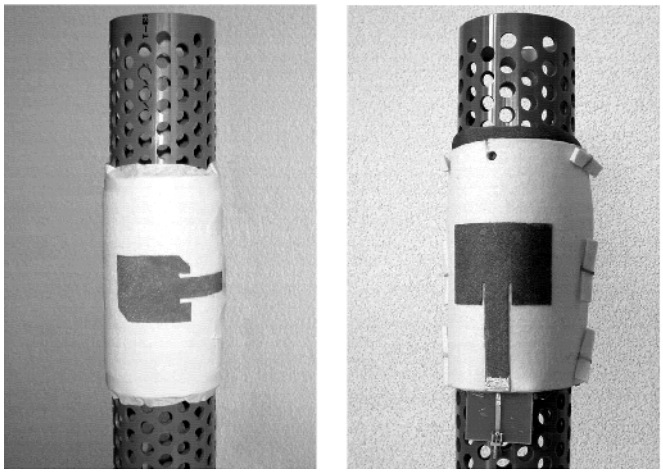

Fig. 12. Bending gauge with 75-mm diameter. (a) Case 1: antenna bent around its x-axis. (b) Case 2: antenna bent around its y-axis.

to the diameters of a small upper arm and a thick thigh. However, the following subsections only present results of bending measurements conducted with the smaller radius since its effect on the antenna characteristic is much stronger. Fig. 12 shows the bending gauge (75-mm diameter) used in measurements.

B. Antenna Interconnect for Measurements

In order to interconnect the antennas with the measurement equipment, a PCB adapter with two connectors had to be deployed consisting of a surface-mount assembly (SMA) on one side and a special PCB-antenna connector on the other side. This transition actually serves the mechanical purpose of connecting from the PCB substrate to the much thicker fabric substrate as can be seen in the magnified section of Fig 13(a). Second, it electrically contacts the 50-Ω microstrip line of the PCB to the 50-Ω and 75-Ω microstrip feed line on the felt and spacer fabric, respectively. The two connectors on the PCB board can be regarded as discontinuities. In the impedance profile in Fig. 13(b) obtained by time domain reflectometry (TDR), we can easily identify all parts of the interconnect, from the SMA connector over the 50-Ω line on the PCB, through the PCB–antenna connector to the antenna microstrip feed line (here: 75 Ω). Especially, the connection from PCB to the textile substrate introduces a significant discontinuity.

Thus, measured and simulated S_{11} parameters of the antennas cannot simply be renormalized to achieve a good agreement. To remove this discontinuity, we modeled the PCB measurement adapters for the felt and spacer fabric antenna and deembedded them from the S_{11} antenna measurements.

In an actual application, the electronics would directly connect to the antenna without any PCB adapters.

C. Return Loss

The return loss or S_{11} describes the impedance mismatch between feed line and the antenna feed point. In our case, the feed line is the microstrip line and the antenna feed point is located where the insets ends into the antenna patch (see Fig. 8). The return loss is defined as the ratio between the power reflected back from the antenna at the feed point and the power fed to the

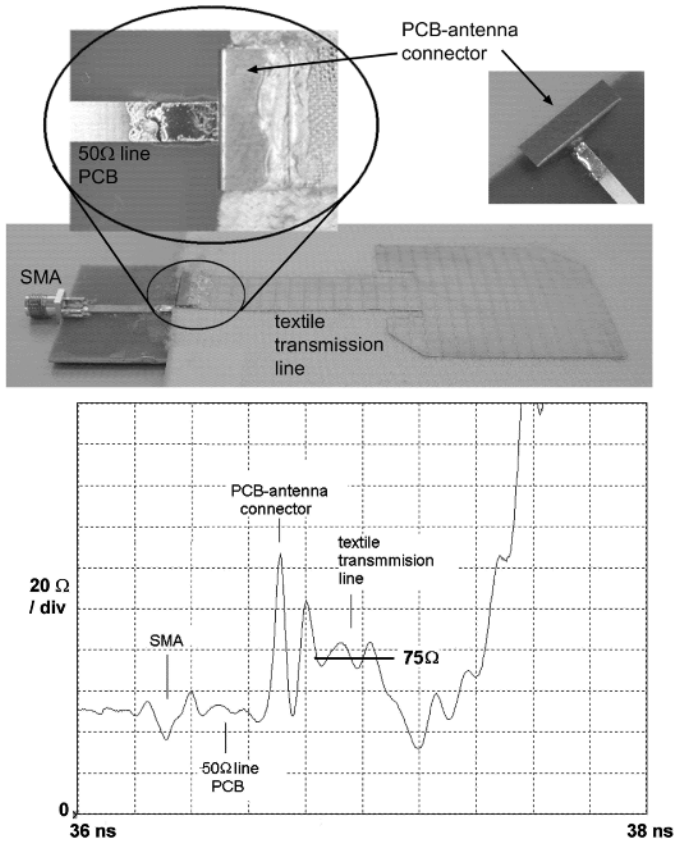

Fig. 13. Measurement of the antenna interconnect. (a) Antenna with PCB measurement adapter and magnified PCB-to-antenna connector. (b) TDR measurement curve of antenna with PCB measurement adapter.

antenna. If the entire power is reflected back, S_{11} will be 0 dB. If the power is completely absorbed by the antenna, the value will be $-\infty$ dB. A low return loss value corresponds to a good matching at a specific frequency.

Fig. 14 shows the measured S_{11} characteristics of the four antennas when kept flat. All antennas except the CS antenna possess good matching and a 10 dB-bandwidth of more than 200 MHz. The CS antenna can be optimized by further adjusting the antenna insets to 75 Ω input impedance. The dielectric losses of the substrates introduce magnitude offsets of -3 dB and -5 dB for the spacer fabric and the felt, respectively. This behavior can be seen best at a frequency of 2 GHz in Fig. 14.

We also conducted S_{11} measurements under defined bending conditions of the antennas. Fig. 15 shows the change of the resonance frequency notch as a function of the bending radius. In this section, we focused on the LS and CF antennas for these and the later measurements on antennas under bending condition. Generally, the resonances are shifted towards lower frequencies and the bandwidth becomes smaller when bent, independent of the bending direction. The smaller the bending radius is, the lower the resonance frequency becomes. Bending of a linearly polarized antenna according to case 1 (see Fig. 12) elongates the antenna patch (L becomes bigger) and, therefore, the resonance length. Formula (4) confirms such a behavior. Similarly, bending in case 2 widens the antenna patch whereby (3) predicts a lowered resonance frequency. The reaction of the CF antenna on bending is complex to predict since both of the two

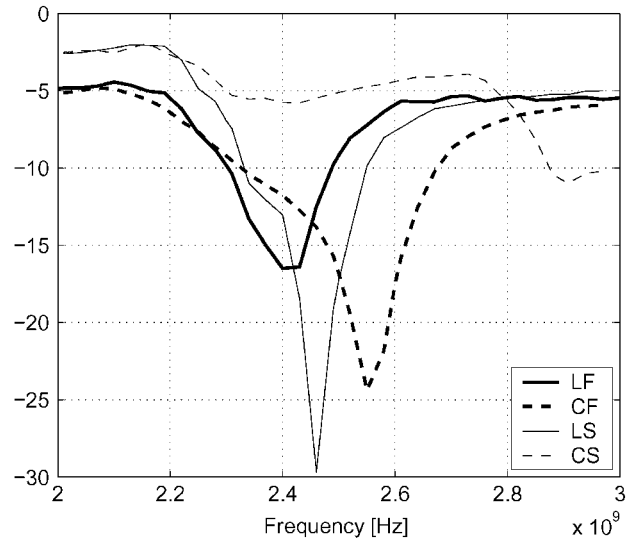

Fig. 14. Measured S_{11} of the four planar antennas.

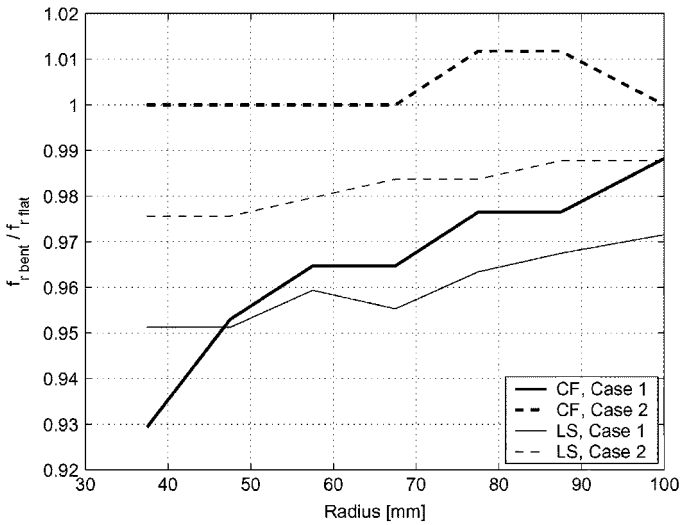

Fig. 15. Measured resonance frequency $f_{r\,\mathrm{bent}}$ as a function of bending radius normalized to the resonance frequency $f_{r\,\mathrm{flat}}$ of the flat antenna. Bending axes correspond to the two cases given in Fig. 12.

orthogonal radiation components change when bent in case 1 and case 2. In case 1, the CF antenna performs like the LS antenna, whereas the resonance frequency shows high immunity against bending in case 2.

D. Radiation Patterns

A radiation pattern characterizes the variation of the radiated far-field intensity of an antenna as an angular function at a specific frequency. Usually, they are shown as cuts along the XZ and YZ planes according to the coordinate system given in Fig. 8. The simulated and measured radiation patterns of two of the four antennas at 2.4 GHz are plotted in Figs. 16 and 17 for the two orthogonal planes XZ and YZ. The measurements agree well with the simulation results. We observe only small differences, which are probably caused by manufacturing imperfections. The CP antennas show good left-handed circular polarization properties (only the figures for the CF antenna are

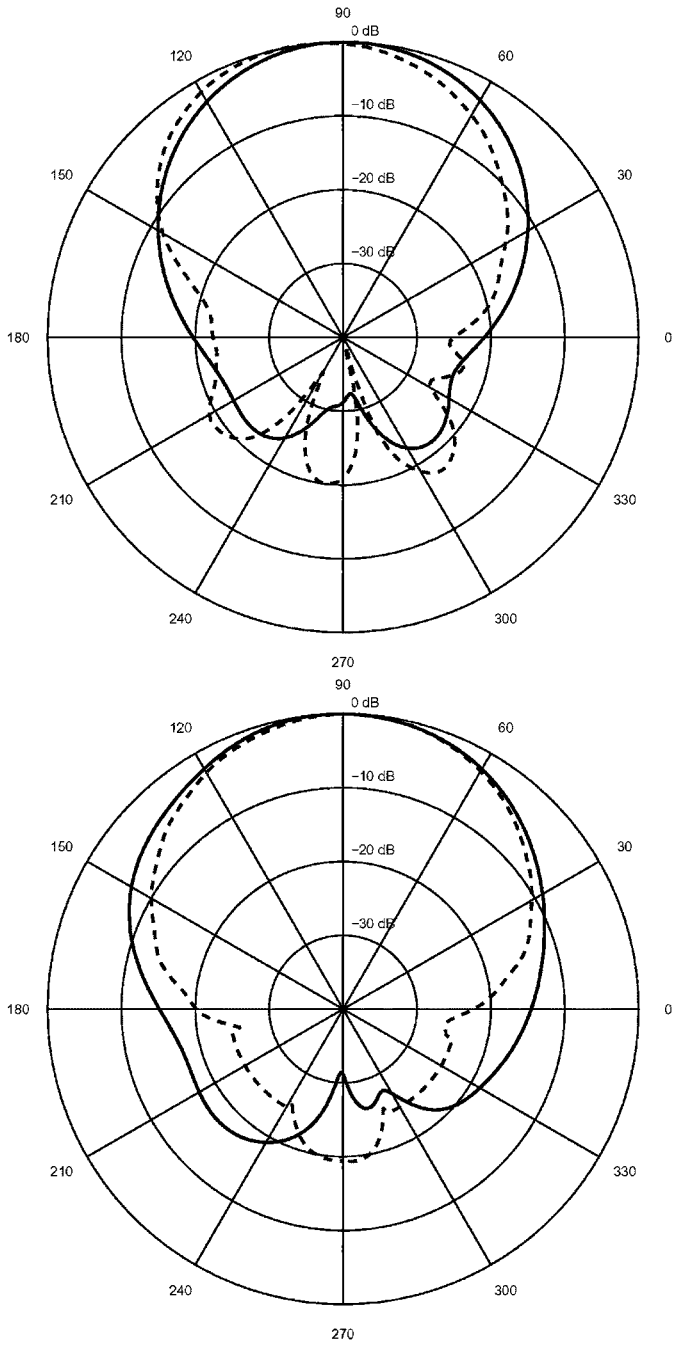

Fig. 16. Simulated (solid) and measured (dashed) radiation pattern (copolarization component) of LS antenna at 2.4 GHz. (a) XZ plane. (b) YZ plane.

depicted). The results of the CP antennas should especially be appreciated since the current distribution in the two orthogonal directions is not obvious in the actual conductive textiles (see Fig. 4). In the design process, we assumed isotropic parameters for the materials, which simplifies the actual inner structures of the materials. Our results prove that this assumption is reasonable.

Since small bending radii show bigger effects on the antenna characteristic, we focused on radiation pattern measurements of bent antennas using the bending gauge with a radius of 37.5 mm as shown in Fig. 12. Second, we only measured the LS antenna and the CF antenna in the two bending directions. The

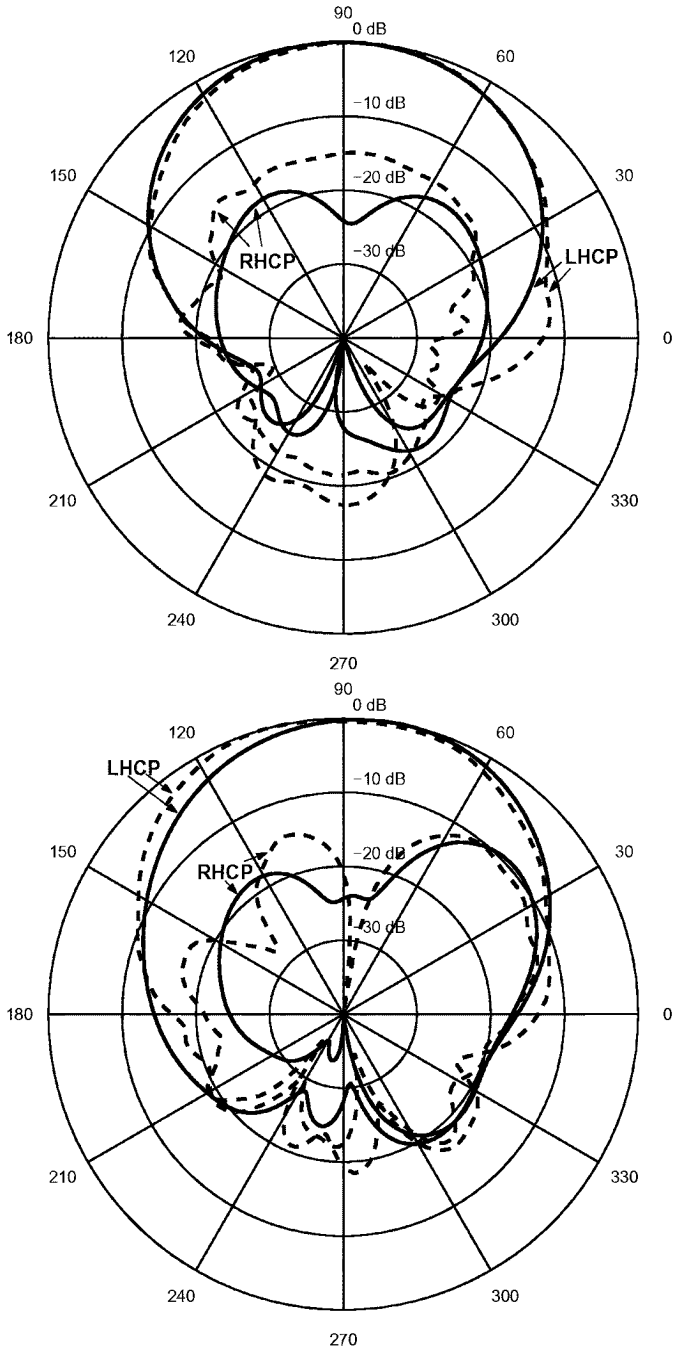

Fig. 17. Simulated (solid) and measured (dashed) radiation pattern (co- and cross-polarization components) of CF antenna at 2.4 GHz. (a) XZ plane. (b) YZ plane.

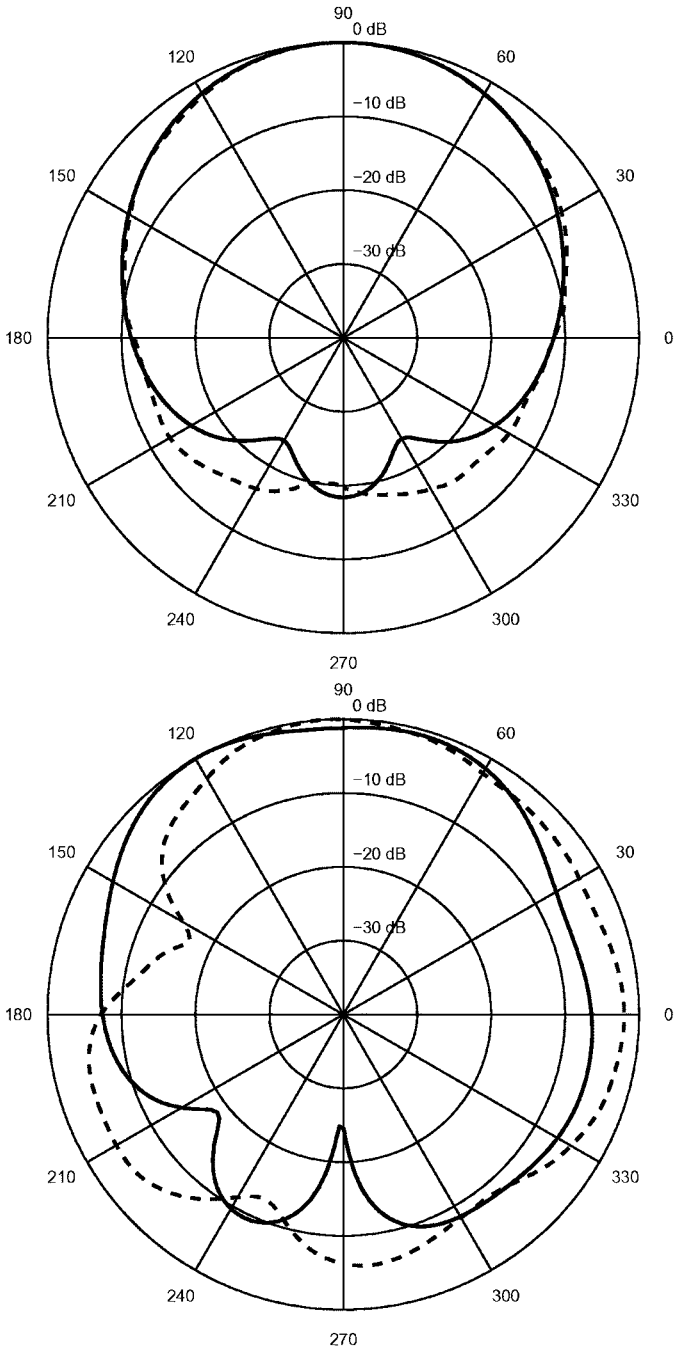

Fig. 18. Simulated (solid) and measured (dashed) radiation pattern (only co-polarization component) of bent LS antenna (radius 37.5 mm) at 2.4 GHz. (a) XZ plane, bending case 2. (b) YZ plane, bending case 1.

obtained patterns are presented in Figs. 18 and 19, respectively. We can see that the bent antenna patterns are less directional for both antennas as compared to their patterns in flat shape. Second, bending according to case 1 shows bigger influence on the radiation patterns than bending in case 2. Table IV compares the half-power beamwidths of the antennas in flat and bent shape. The half-power beamwidth is the angle between the two points (on the same plane) at which the radiation falls to half (-3 dB) of the maximum power (normalized to 0 dB). Evident is the increased level of back-radiation resulting from decreased shielding due to ground plane bending.

In case of the CF antenna, we observe a degradation of CP performance, i.e., higher level of the cross-polarized RHCP component. This result is, however, not surprising since it is a circularly polarized antenna. Bending of the antenna changes the amplitude and the phase relations between the two orthogonal current modes present in the circularly polarized antenna. In our experiments, we have noticed that the phase relation between two modes is sensitive to bending of the antenna.

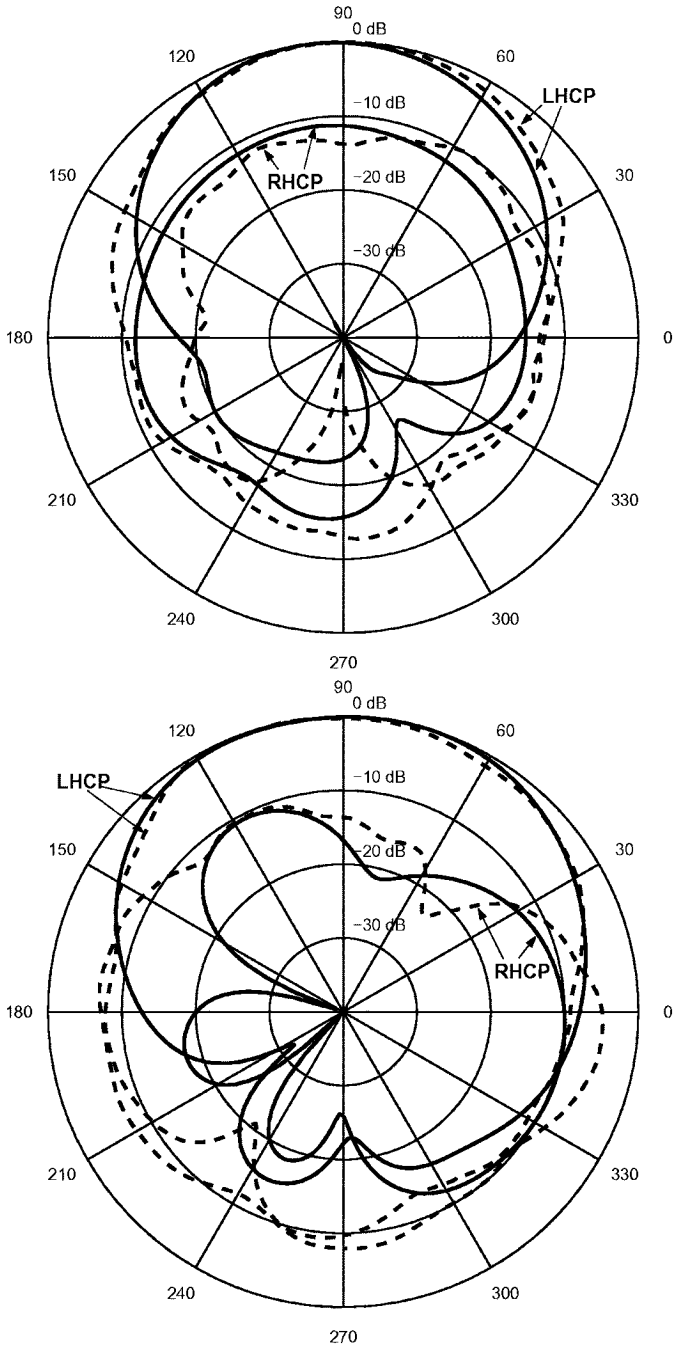

Fig. 19. Simulated (solid) and measured (dashed) radiation pattern (co- and cross-polarization components) of bent CF antenna (radius 37.5 mm) at 2.4 GHz. (a) XZ plane, bending case 2. (b) YZ plane, bending case 1.

TABLE IV
MEASURED HALF-POWER BEAMWIDTH OF LS AND CF ANTENNA

Configuration	LS	CF
XZ plane, Flat	57^o	73^o
YZ plane, Flat	62^o	75^o
XZ plane, Case 1	78^o	82^o
YZ plane, Case 2	87^o	100^o

Additionally, textile material properties such as permittivity slightly change due to the bending that influences the current distributions on the antenna as well. In case of linearly polarized antennas, bending does not have a significant impact on the polarization purity since only one current mode (distribution) is present in the antenna.

TABLE V
GAIN OF LF ANTENNA VARIANTS AT 2.4 GHZ CONSIDERING DIFFERENT LOSS SOURCES

Lossy Substrate	Conductive material: Knitted Fabric 2) G_{eff} [dBi]	η [%]	Copper foil G_{eff} [dBi]	η [%]
-	5.5	44.9	9.0	99.0
√	4.4	34.7	7.5	69.0

E. Effective Antenna Gain

The gain of an antenna describes the amplification of the microwave signal at a specified frequency in a particular direction compared to the isotropically radiating antenna. The effective antenna gain is not only determined by the antenna shape, but also by the applied materials. The effects of the material choice on the antenna gain have been investigated using Ansoft HFSS simulations [19]. For the simulations, we chose the LF antenna with the dielectric losses of $\tan\delta = 0.02$ and the sheet resistance of about 1 $\Omega/\square$ as a basis. We run antenna simulations with and without including the dielectric loss of the felt as well as with the knitted fabric 2) and with copper foil as conductive planes.

Table V lists antenna gains G_{eff} and efficiencies η of the simulated variants at 2.4 GHz, whereas the lossy variant with the knitted fabric 2) agrees with the real LF antenna gain measurement in the anechoic chamber. The effective gain is defined as $G_{\text{eff}} = \eta \cdot G$, where G is the antenna gain. In the first row of Table V, η includes only the conductive losses and in the second row, η contains the dielectric and the condictive losses together.

If we assume a link between the real LF antenna ($G_{\text{eff}} = 4.4$ dB) and an external antenna of any type, the conductive losses of the LF antenna already reduce the communication range by about 30% compared to an LF antenna with copper foil ($G_{\text{eff}} = 7.5$ dB). Comparing the best variant ($G_{\text{eff}} = 9.0$ dB) with the real LF antenna, a range drop by 40% occurs. This calculation is based on the Friss transmission formula [16] assuming a given receiver sensitivity.

F. Axial Ratio (AR)

The axial ratio is a parameter to describe either elliptical or circular polarization [16]. It is defined as the ratio of the major to the minor axis of the polarizations ellipse of an antenna. To achieve circular polarization, the field vector (electric or magnetic) must fulfill the following conditions:

1) the field must have two orthogonal linear components;
2) the two components must have the same magnitude;
3) the two components must have a time-phase difference of odd multiples of 90°.

In the ideal case, AR would be equal to 1 (or 0 dB). In practice, it is difficult to achieve $\text{AR} = 1$, especially for a wide frequency band and for a broad range of spatial directions of antenna propagation. Thus, an antenna is usually regarded to be CP when its axial ratio stays below 3 dB for a given direction of propagation.

We extracted the AR from our simulated and measured radiation patterns of LHCP and RHCP field components for the

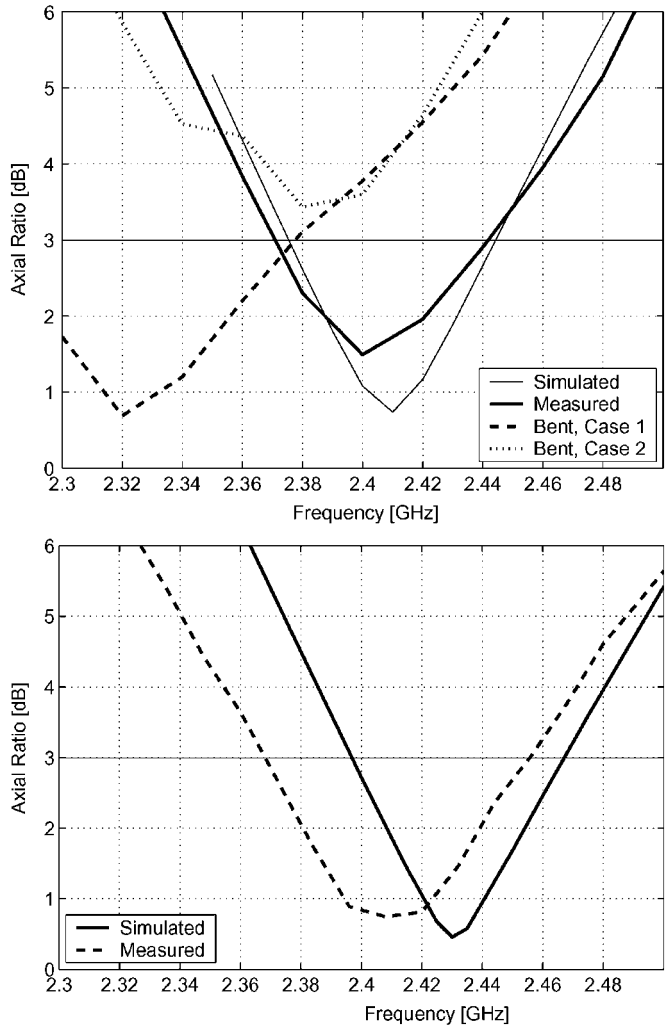

Fig. 20. Simulated and measured axial ratios (decibels) of CF and CS Antenna. (a) CF antenna, flat and bent. (b) CS antenna, flat.

circularly polarized antennas (CF and CS). The AR was computed using (5)

$$\mathrm{AR} = \frac{\mathrm{LHCP} + \mathrm{RHCP}}{\mathrm{LHCP} - \mathrm{RHCP}} \tag{5}$$

It is evident that AR reaches infinity when LHCP and RHCP are equal meaning that the antenna is linearly polarized. In Fig. 20, we can see the comparison between simulated and measured AR in the direction of maximum radiation for the CF and CS antennas.

Additionally, we were interested in the effect of bending on the axial ratio. Again, we concentrated on the radius of 37.5 mm and the CF antenna. Fig. 20(a) also includes the bent measurements of the CF antenna. Bending pushes the axial ratio curve towards lower frequencies by about 80 MHz and abolishes circular polarization at all, respectively. In addition, bending in case 1 broadens the bandwidth of the axial ratio as can be verified in Table VI.

TABLE VI
MEASURED BANDWIDTH OF AXIAL RATIO FOR CF AND CS ANTENNA

Antenna	Measured BW [MHz]	[%]	Bending Radius [mm]
CS	88	3.65	∞
CF	71	2.96	∞
CF	100	4.3	$37.5mm$, Case 1
CF	no CP		$37.5mm$, Case 2

VII. CONCLUSION

We have shown that standard antenna design techniques perform well even for textile substrates and conductive textiles. The antennas presented not only feature good properties, but also are easy to manufacture. They satisfy Bluetooth specifications even when bent down to radius of 37.5 mm and mounted according to case 2 Fig. 12(b). Generally, S_{11} and radiation pattern show better robustness against bending in case 2 whereas the axial ratio is more sensitive in this configuration. Bending causes a similar impact on the characteristic of linearly and circularly polarized antenna, though, circularly polarized antennas lose their CP property at the specified center frequency (2.4 GHz).

The choice of a knitted or a woven conductive textile for antennas depends on the application and its favored deformation behavior. In our investigations, we could see that mechanical stabilization is essential to preserve the desired antenna characteristic. This requirement can either be satisfied by using a stable (nonknitted) substrate such as the felt or by using a stable (nonknitted) patch/ground plane.

In general, commercial ceramic Bluetooth antennas [20] radiate in omnidirectional patterns making them available for universal applications. They feature bandwidths in the range of 150 MHz, similar to our antennas. However, antennas in wearable applications need directivity in order to avoid unnecessary radiation exposure to the human body and radiation losses. Our textile patch antennas provide this desired directivity.

While we tried to understand the effects of bending on the antennas in this paper, we will investigate the effects of human body proximity in the future. We will conduct simulations with human phantom models as well as measurements with real humans.

For applications purposes, the final goal is to mount the critical RF components on the textile substrate itself close to the antenna patch. To achieve this goal, the two fields of textile packaging [4] and textile antennas need to merge.

ACKNOWLEDGMENT

The authors would like to thank Mr. Benedickter for the extensive antenna measurements. They also thank their Ph.D. colleague C. Mattmann for providing the resistance data in dependence of strain.

REFERENCES

[1] S. Mann, "On the bandwagon or beyond wearable computing," *Personal Technol.*, vol. 1, no. 4, pp. 203–207, 1997.
[2] *Specification of the Bluetooth System, Radio Specification*, [Online]. Available: http://www.bluetooth.org., Bluetooth SIG
[3] S. Brebels, J. Ryckaert, B. Cme, S. Donnay, W. D. Raedt, E. Beyne, and R. P. Mertens, "Sop integration and codesign of antennas," *IEEE Trans. Adv. Packag.*, vol. 27, no. 2, pp. 341–351, May 2004.

[4] I. Locher, T. Kirstein, and G. Tröster, "Routing methods adapted to e-textiles," in *Proc. 37th Int. Symp. Microelectron. (IMAPS 2004)*, Nov. 2004.
[5] D. Cottet, J. Grzyb, T. Kirstein, and G. Tröster, "Electrical characterization of textile transmission lines," *IEEE Trans. Adv. Packag.*, vol. 26, no. 2, pp. 182–190, May 2003.
[6] P. Salonen, M. Keskilammi, and M. Kivikoski, "Single-feed dual-band planar inverted-f antenna with u-shaped slot," *IEEE Trans. Antennas Propag.*, vol. 48, no. 8, pp. 1262–1264, Aug. 2000.
[7] P. Massey, "Mobile phone fabric antennas integrated within clothing," in *Proc. 11th IEE Conf. Antennas Propag. (IEE Conf. Pub. No. 480)*, Apr. 2001, vol. 1, pp. 344–347.
[8] M. Tanaka and J. Jae-Hyeuk, "Wearable microstrip antenna," in *Proc. IEEE Antennas Propag. Soc. Int. Symp.*, June 2003, vol. 2, pp. 704–707.
[9] P. Salonen and H. Hurme, "A novel fabric wlan antenna for wearable applications," in *Proc. IEEE Antennas and Propagation Soc. Int. Symp.*, Jun. 2003, vol. 2, pp. 700–703.
[10] P. Salonen, Y. Rahmat-Samii, H. Hurme, and M. Kivikoski, "Dual-band wearable textile antenna," in *Proc. IEEE Antennas Propag. Soc. Int. Symp.*, Jun. 2004, vol. 1, pp. 463–466.
[11] M. Klemm, I. Locher, and G. Tröster, "A novel circularly polarized textile antenna for wearable applications," in *Proc. 34th Eur. Microw. Week*, Oct. 2004, pp. 137–140.
[12] *P130 Technical Data Sheet*, [Online]. Available: http://www.statex.de., Statex Produktions & Vertriebs GmbH, Bremen, Germany
[13] *Nora Technical Data Sheet*, [Online]. Available: http://www.statex.de., Statex Produktions & Vertriebs GmbH, Bremen, Germany
[14] J. Grzyb, I. Ruiz, and G. Tröster, "An investigation of the material and process parameters for thin-film MCM-D and MCM-L technologies up to 100 GHz," in *Proc. 53rd Electron. Compon. Technol. Conf. (ECTC2003)*, New Orleans, LA, May 2003, pp. 478–486.
[15] A. Carullo, A. Ferrero, and M. Parvis, "A microwave system for relative humidity measurement," in *Proc. 16th IEEE Instrum. Meas. Technol. Conf. (IMTC)*, May 1999, vol. 1, pp. 124–129.
[16] C. A. Balanis, *Antenna Theory: Analysis and Design*, 2nd ed. New York: Wiley, 1996.
[17] C.-K. W. W.-Sh. Chen and K.-L. Wong, "Inset microstripline-fed circularly polarized microstrip antennas," *IEEE Trans. Antennas Propag.*, vol. 48, no. 8, pp. 1253–1254, Aug. 2000.
[18] *HFSS*, [Online]. Available: http://www.ansoft.com/products/hf/hfss/, Ansoft Corp., Pittsburgh, PA.
[19] *Ansoft HFSS User Manual*, , 2002, Ansoft Corp., Pittsburgh, PA..
[20] *ANT-2.45-CHP Technical Data Sheet*, [Online]. Available: http://www.antennafactor.com, Antenna Factor, Inc., Grants Pass, OR.

Ivo Locher (S'01) received the B.Sc. degree with a thesis about MSK transmitters/receivers including their realization in hardware using Xilinx FPGAs in 1997 and the M.Sc. degree in electrical engineering in the field of signal processing with focus on speech processing under Prof. Alwan and Prof. Srivastava from the University of California, Los Angeles (UCLA), in 2002. He is currently pursuing the Ph.D. degree at ETH Zurich, Zurich, Switzerland.

Before going to UCLA, he was Research Assistant for telecommunications under Prof. Portmann at the University of Applied Science, Lucerne, Switzerland. His research interests include e-textiles and wearable computing with a focus on textile packaging and textile antennas.

Mr. Locher received Second Prize in the DAC Student Design Contest in June 2002.

Maciej Klemm received the M.Sc. degree in microwave engineering from Gdansk University of Technology, Gdansk, Poland, in 2002. He is currently pursuing the Ph.D. degree in the Electronics Laboratory, Swiss Federal Institute of Technology (ETH) Zurich, Switzerland.

His current research interests include UWB antennas and communications, antennas interactions with a human body, electromagnetic simulations, microwave MCM technologies, and millimeter-wave integrated passives. In the spring of 2004, he was a Visiting Researcher at the Antennas and Propagation Laboratory, University of Aalborg, Aalborg, Denmark, where he was developing new antennas for UWB radios.

Mr. Klemm was awarded the Young Scientists Content Award at the IEEE MIKON 2004 conference for his paper about antennas for UWB wearable radios.

Tünde Kirstein received the M.S. degree in clothing technology from the University of Applied Sciences, Hamburg, Germany, in 1996 and the Ph.D. degree in mechanical engineering from the Dresden University of Technology, Dresden, Germany, in 2001.

She was a CAD Engineer with Th. Braun (clothing industry), Hamburg, Germany, from 1995 to 1997 and a Lecturer for pattern construction at the Fashion Design Academy, Hamburg, from 1996 to 1997. She worked at the Institute of Textile and Clothing Technology, Dresden, while pursuing the Ph.D. degree. In 2001, she joined the Wearable Computing Laboratory, Swiss Federal Institute of Technology (ETH), Zürich, Switzerland, where she is in charge of the Smart Textiles Group.

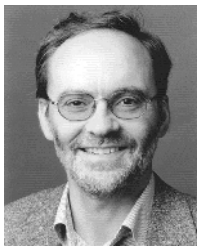

Gerhard Tröster (SM'93) received the M.S. degree from the Technical University Karlsruhe, Karlsruhe, Germany, in 1978 and the Ph.D. degree from the Technical University of Darmstadt, Germany, in 1984, both in electrical engineering.

He is a Professor and head of the Electronics Laboratory, Swiss Federal Institute of Technology (ETH), Zürich, Switzerland. During the eight years he spent at Telefunken Corporation, Germany, he was responsible for various national and international research projects focused on key components for ISDN and digital mobile phones. His field of research includes wearable computing, reconfigurable systems, signal processing, mechatronics, and electronic packaging. He authored and coauthored more than 100 articles and holds five patents. In 1997, he cofounded the spinoff U-Blox AG.